Biophys Struct Mech (1981) 8: 1–22

Biophysics of Structure and Mechanism

Review

Hydromechanics and Biology

W. Nachtigall

Universität des Saarlandes, Fachbereich 16: Biologie, Fachrichtung: Zoologie, D-6600 Saarbrücken, Federal Republic of Germany

Summary. To exemplify relations between biology and hydrodynamics the Reynolds number range and the effects of viscosity and inertia in swimming and flying organisms is discussed. Comparing water beetles and penguins it is shown, that the technical drag coefficient is an adequate means to describe flow adaptation in animals. Compared to technical systems, especially the penguins' drag coefficient is astonishingly low. Furthermore, the question, why comparatively thick bodies in penguins and dolphins show rather low drag is discussed. Distributed boundary layer damping in dolphins and secretion of special high molecular slimes in fishes help to keep flow characteristics laminar. As an example of one easily understood thrust mechanism, the drag inducing pair of rowing legs in water beetles is morphologically and hydrodynamically analysed. Fish swimming is discussed as a locomotion principle using lift components. Thrust generation by the moving tail fin of a fish is analysed in detail. Coming back to the influence if Reynolds number, it is finally shown, how very small, bristle bearing swimming legs and wings of insects make use of viscosity effects for locomotion.

Key words: Hydrodynamics – Locomotion – Swimming – Thrust generation – Flow adaptation

The wide range of interlacing disciplines in biochemistry and biophysics has greatly enriched scientific research by bringing together the knowledge of specialists of widely differing attitudes. In the following, the co-operation between biology and technical sciences dealing with the biophysical aspects of movement physiology will be demonstrated by means of a series of examples with special attention being given to that of hydromechanics. Only the flow of fluids around bodies will be studied and not the flow in tubes (blood vessels) since the latter present quite unique problems.

In the classification of biological flyers and swimmers, a dimensionless number used in engineering has been proved to be extremely important. This

0340-1057/81/0008/0001/$ 04.40

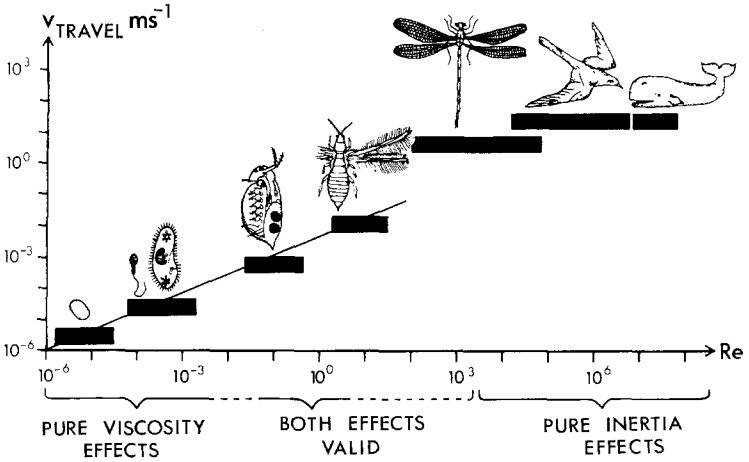

Fig. 1. Travelling speed v_{travel} of biological objects as a function of the Reynolds number Re. According to Nachtigall (1977)

number is the Reynolds number Re = vl ν^{-1} (v velocity between object and surrounding medium, 1 characteristic length of object, ν kinematical viscosity of the medium, equal to the quotient from viscosity and density). Dimension calculations have shown that this Reynolds number gives the relationship between the forces of inertia and the forces of friction or viscosity. Figure 1 shows the average travelling speeds of organisms plotted as a function of the Reynolds number. The Re-range of biological objects lies between 10^{-6} (bacteria) and 10^8 (large whales). The span reaches the astronomical value of 10^{14} and is valid for the range of almost pure state viscosity effects in the smallest organisms to the range of almost pure states of inertia effects in the largest swimmers. If the ciliary movement of a ciliate were to cease, the animal would come to an abrupt halt because the effects of inertia have no influence in this case. Contrary to this, large whales, dolphins, seals, penguins, and fish will continue to advance for several meters or at least fractions of a meter in smaller animals before coming to a halt because the effects of inertia are dominant. This behaviour enables one to determine, without disturbing the animal in any way, the flow adaptability of such animals and will be explained further on. This is important because the hydro- or aerodynamical balances normally used in measuring drag are disturbing factors even when one can reduce them to a minimum by suitable experimental constructions. For example, how good is the flow adaptation of a water beetle's body?

The bodies of swimming water beetles and water bugs create almost pure drag, whilst the rear legs act as paddles. Figure 2 shows the bodies of several species of dytiscid beetles. The degree of efficiency of flow adaptation can be expressed as the dimensionless coefficient of drag $c_d = d/A \cdot q$ (d drag, A area, q pressure head) = $0{,}5\,\varrho\, v^2$ (v velocity, ϱ density). In order to calculate the so-called frontal area coefficient of drag, c_{dS}, which is characteristic for cars, one uses the frontal area of the object as reference area. This is the area in which the

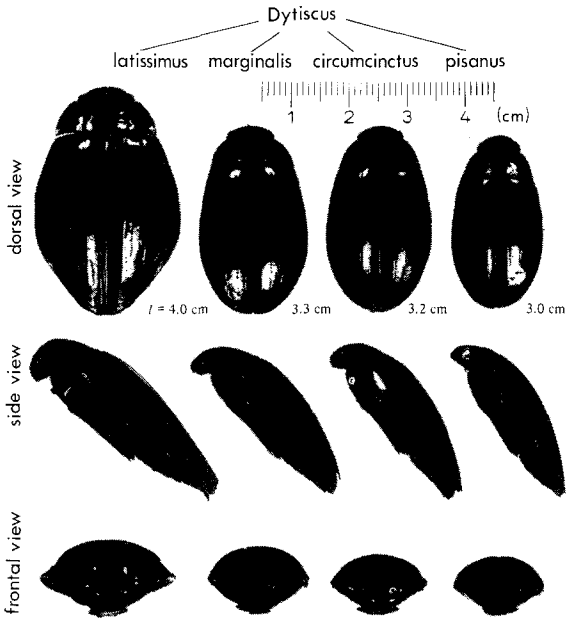

Fig. 2. Bodies of several carnivorous water beetles (*Dytiscidae*), seen from three directions of space. According to Nachtigall (1980)

projected body appears when one uses parallel projection onto a plane perpendicular to the direction of movement. The smaller the coefficient, the less power is required to keep a body in steady motion if A and q are equal. c_d is a function of Re. The coefficients for all common technical shapes and the Re – ranges are known. This presents the biologist with an ideal testing instrument, e.g., if he knows the extreme c_d values in the Reynolds numbers range of his water beetle (Re $\approx 10^3$), i.e., the smallest and greatest possible values, then he can tabulate his biological data in a scale, the beginning (best value) and end (poorest value) of which are known. In this way he receives a precise answer to the question on the 'quality' of his biological construction. Water beetle bodies with given frontal area A, were tested in water canals and wind tunnels by the author; d was measured by means of hydro- or aerodynamic balances, v by flow probes. Figure 3a shows the mean c_{dS} values for different Dytiscus-species, presented in Fig. 2. These values are plotted between the technically best and poorest values. It is shown that the coefficients lie close to the minimum, and far from the maximum value. Thus it can be said that the bodies have an optimal hydrodynamical shape. They do not reach absolute minimum values, a fact which has a very plausible explanation: "drop" shaped "ideal" bodies are hydrodynamically unstable; at the slightest oblique flow they would turn sideways. Stabilizing structures on the other hand will enlarge, i.e., worsen the coefficient. This can also be tested with dytiscid bodies. If one carefully files away the elongated edges of the prothoracic plate and elytral margins of *Dytiscus marginalis* or *Dytiscus latissimus,* the coefficient decreases (Fig. 4). One may assume that water beetle bodies have evolved highly proficient hydrodynamical shapes just within the limits of swimming stability.

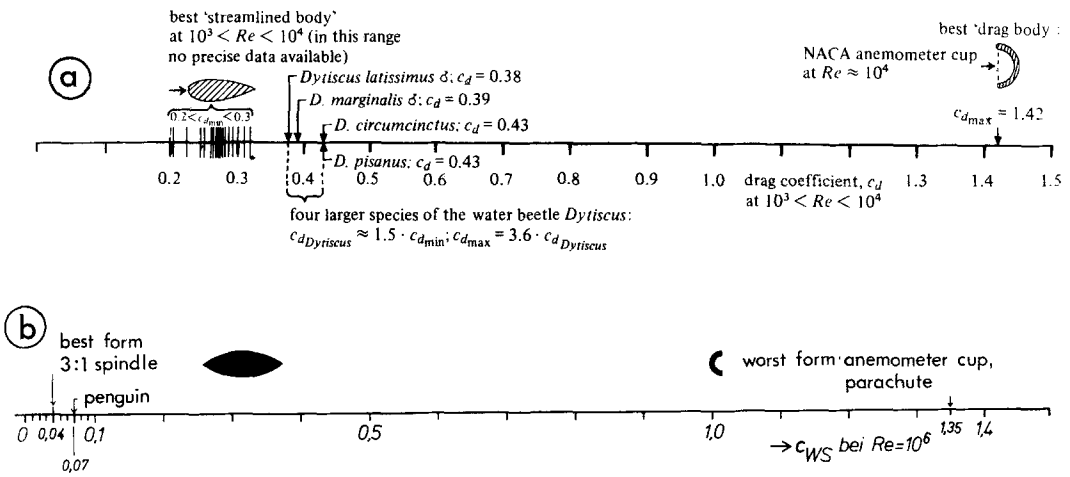

Fig. 3. a Frontal area drag coefficient in the water beetles shown in Fig. 2, plotted on a scale between technical extreme values at $Re \approx 10^3$. **b** Frontal area drag coefficient in the Gentoo penguin, *Pygoscelis papua,* plotted on a scale between the technical extreme values at $Re \approx 10^6$. **a** and **b** According to Nachtigall (1980) and Nachtigall and Bilo (1980), respectively

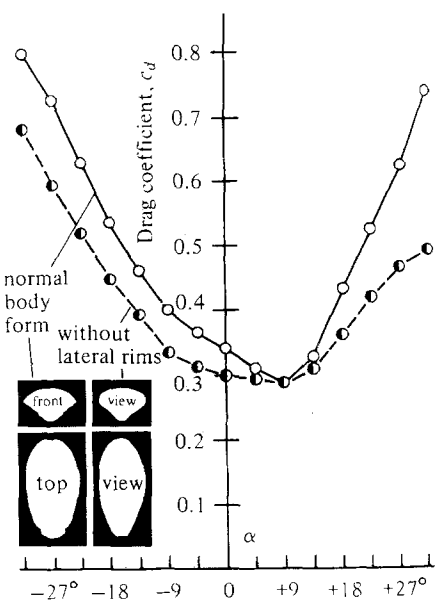

Fig. 4. Frontal area drag coefficient c_{dF} in Dytiscus marginalis ♂ with and without prothoracic and elytral edges (compare inserted photos) at $Re \approx 10^3$ as a function of the angle of attack α between the longitudinal axis of the body and the direction of flow. According to Nachtigall and Bilo (1965)

It is quite impossible to study swimming vertebrates with the balance method described above. One cannot suspend a fish, penguin, or seal from a drag balance. Therefore, Dietrich Bilo and I have developed a new method permitting one to calculate the c_d value from the kind of body movement delay after an accelerating beat, i.e., during passive deceleration. We began by filming the penguin Pygoscelis papua in a penguinarium. From these films we calculated

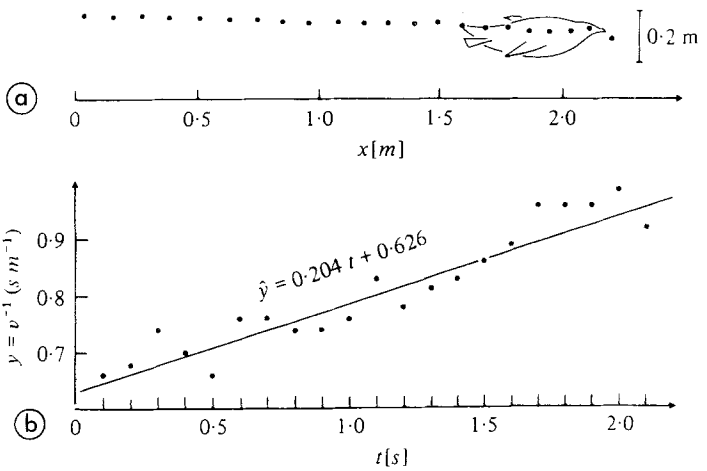

Fig. 5. a Distance – time – function of a Gentoo penguin, Pygoscelis papua, during "gliding out". **b** Regression line through the points from $v^{-1}(t)$ obtained by analysing a. According to Bilo and Nachtigall (1980)

distance time-functions during undisturbed deceleration by means of an analysing projector and single frame analysis. An example is given in Fig. 5a. If one uses the differential equation to the second power for the force of inertia during deceleration, then $\dot{v}(t) = -a\varrho\, v^2(t)$ with a = 0.5 $c_{dF} A\, m^{-1}$ (v speed, A frontal area, ϱ density, m animal mass). The integration of this differential equation gives the result $v(t) = 1\,(c + at)$ with a starting speed of $v_0 = 1/c$. If one replaces $y(t)$ with $v^{-1}(t)$ in the equation $y(t) = at + c$, one can calculate c_{dF} from the gradient a by means of linear regression when A, ϱ, and m are known (Fig. 5b). Using this method on *Pygoscelis papua,* the surprisingly low value of $c_{dF} = 0.07$ was obtained at Re = 10^6 (Fig. 3b). (It might be slightly higher if the virtual mass of the surrounding flow field is taken into account.) This value is much better than anything which technical science can offer in the way of ready made structures (cars, submarines, torpedoes, etc.; Fig. 6) and can only be beaten by purely technical "ideal" forms. These forms, however, are flow-unstable and therefore unsuitable for trunks of ships, aircraft or cars without supplementary stabilizing surfaces. In comparison to this, the penguin is a "complete" form, i.e., it has drag creating supplementary surfaces such as the fin-like frontal extremities and the sideward steering rear extremities. The exceptionally favourable coefficient of this biological construction may not only be due to the apparently optimal shape of the trunk (Fig. 7), but also to the short feather coating. It has been suggested that the latter has turbulence damping properties similar to those proved to be possessed by the special skin structrue of dolphins. The so-called volume drag coefficient c_{dV} may be even more interesting than that of the frontal area, c_{dF} (and surface area c_{dS}, which has been calculated to be 0.004). One can calculate c_{dV} by replacing A with the volume to the power of two thirds ($V^{2/3}$), which shows the dimension of an area. A c_{dV} value smaller than that of another body means that the power to keep this body of a

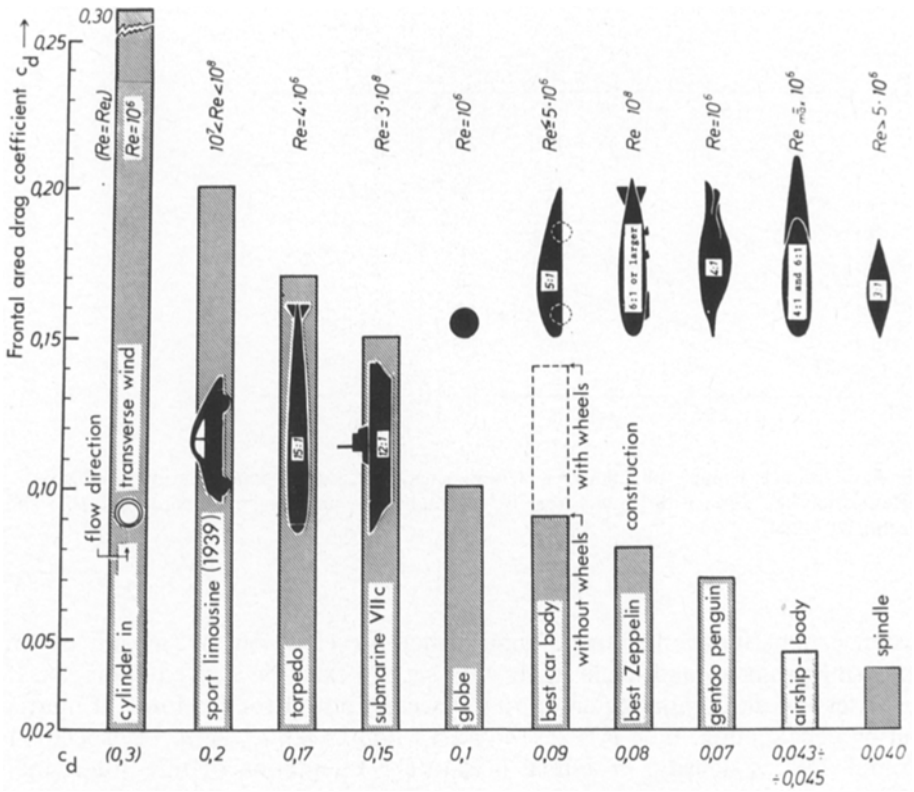

Fig. 6. Examples of technical bodies with small frontal area drag coefficients compared to the Gentoo penguin *Pygoscelis papua.* According to Nachtigall and Bilo (1980)

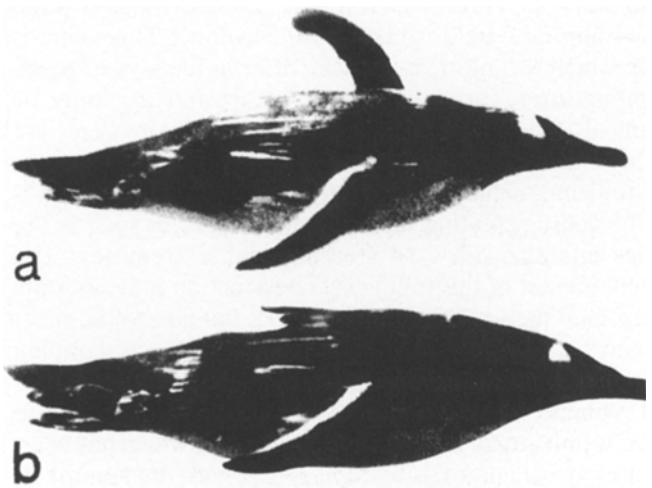

Fig. 7. Gentoo penguin "gliding out", filmed in a penguinarium with a super 8 camera. Original photos by Nachtigall. According to Nachtigall and Bilo (1980)

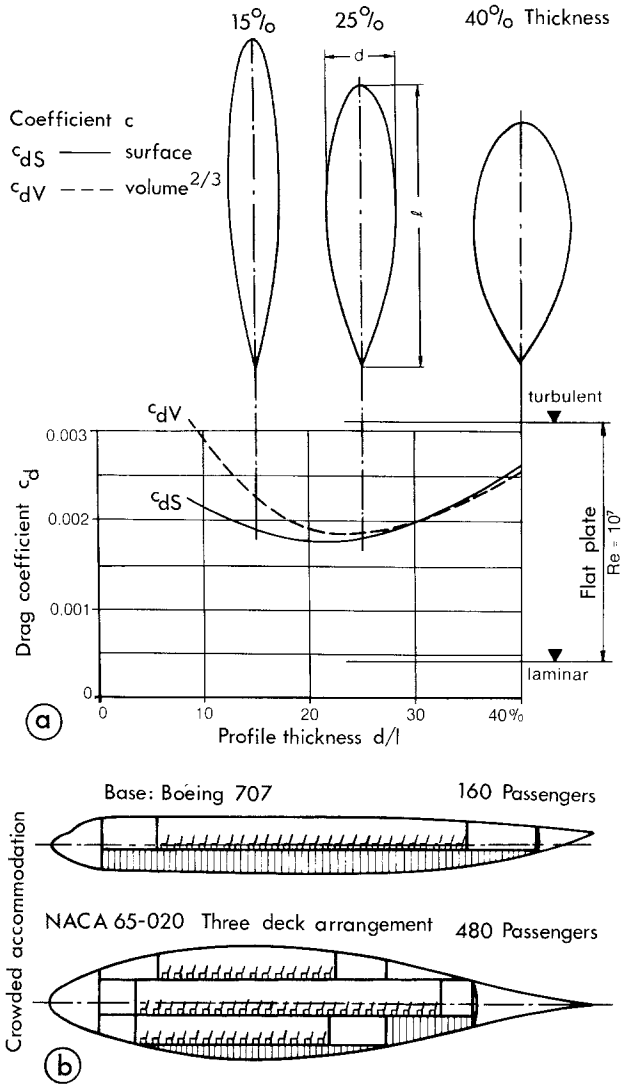

Fig. 8. a Volume and surface drag coefficients c_{dV} and c_{dS} of a low drag body plotted as a function of the relative profile thickness d/l at high Reynolds numbers Re = 10^7. **b** Comparison between a conventional aeroplane body (Boeing 707) and a projected laminar body similar to that found in nature (dolphin body). According to Hertel (1963)

certain volume (i.e., mass) and a given size and speed in motion is smaller than that of the other body. A value of 0.031 was calculated for Pygoscelis which is comparable to that of the aerodynamically favourable shape of an airship. In such forms c_{dV} is minimal at the length – thickness – relation just as it is in swimming penguins, i.e., $l/d \approx 4.5$, which means relatively stocky bodies (Figs. 8 and 9b).

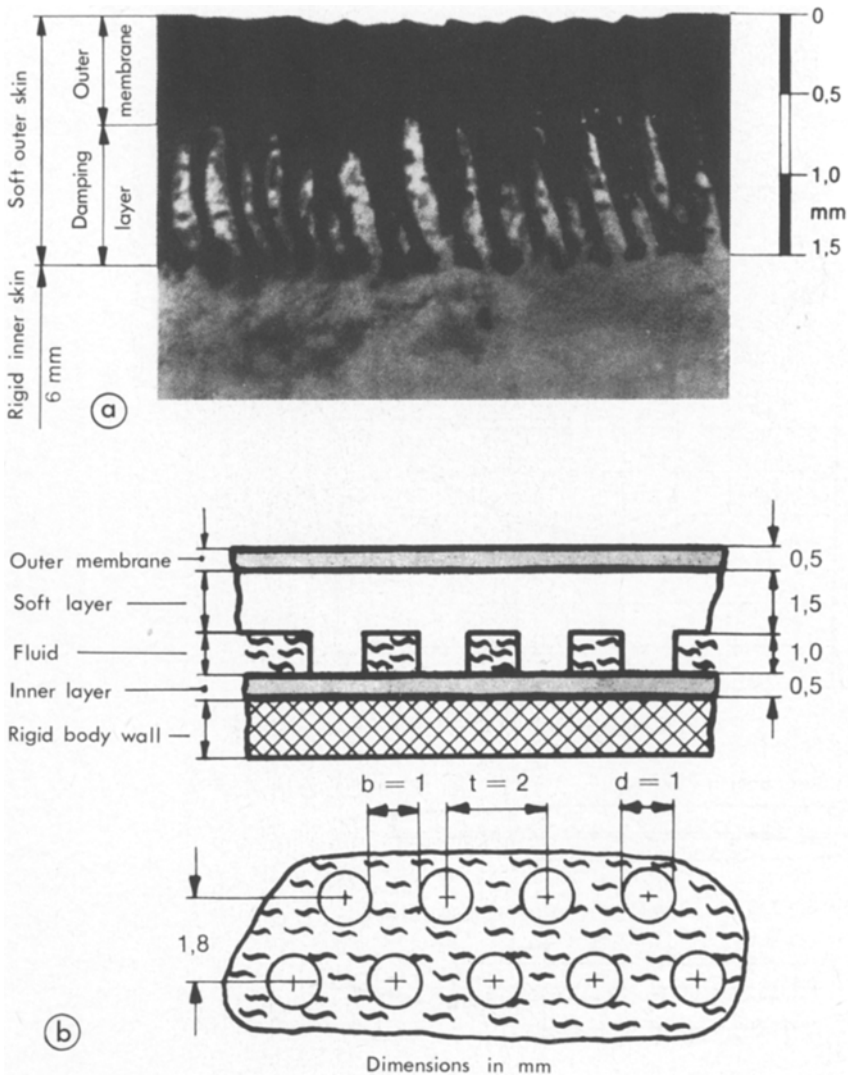

Fig. 9. a Cross-section through the skin of a dolphin, Cephalorhynchus commersonii. **b** Technical model of the dolphin's skin. **c** Flow diagram of the liquid between the rubber nap of the model skin when a pressure wave passes over it. **d** Surface drag coefficient c_{dS} of a rotational body which has been coated with a model skin of carrying rigidity. The limiting curves for totally laminar and totally turbulent boundary layers of the flat plate are indicated. According to Kramer (1960)

A biological paradox, discovered in the 1930's by the English physiologist Sir James Gray, has been a theme for discussion ever since. A dolphin can swim much more quickly than its muscle mass really seems to permit. In other words, to achieve the high speed of swimming recorded, a dolphin has to produce six times as much power as its muscles are capable of generating if it were as stiff

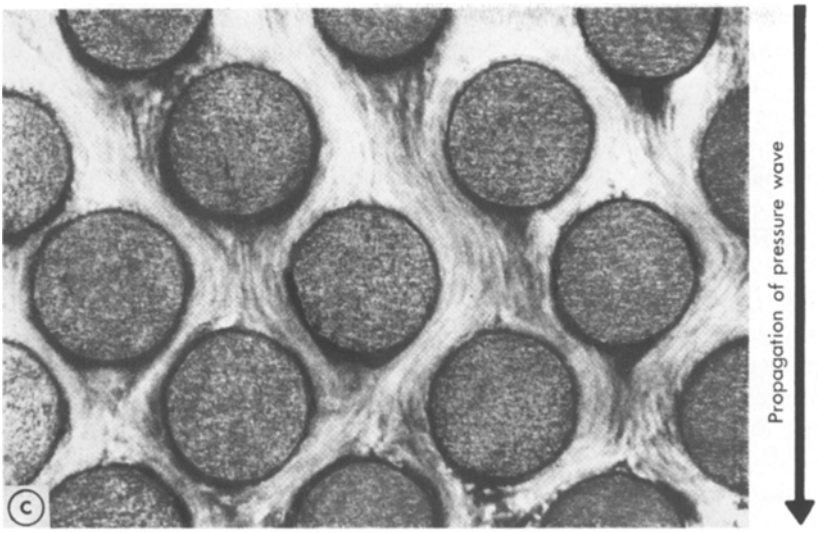

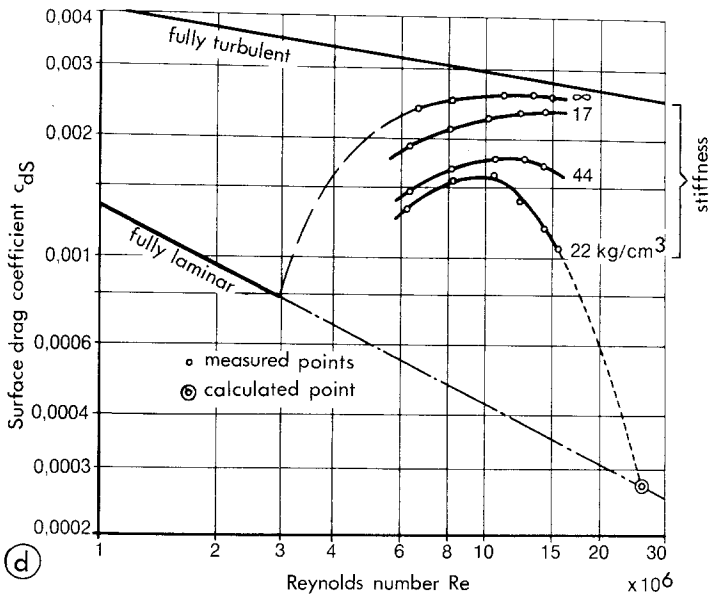

Fig. 9c and d. Legend see page 8

technical form. A dolphin must therefore produce much less drag than a technical object of exactly the same shape. After the second world war, the aerodynamicist M. O. Kramer created the hypothesis that perhaps the extraordinary structure of a dolphin's skin was responsible for this phenomenon. The skin consists of a 2–3 mm thick inner skin, a very loose, mesh – like tissue with

muscular and connective tissue – like structures and finally, a 1.5 mm thick outer skin which has an extremely loose and spongy tissue consisting of up to 80% water. The inner skin has numerous cone – like projections called corium papilles which reach like arrows to touch the outer skin (Fig. 9a). Kramer built an artificial dolphin skin from a sheet of rubber with protrusions (Fig. 9b), the cavities of which were filled with a viscous liquid which was free to flow back and forth (Fig. 9c). Flow around steel plates and rotationally symmetrical bodies becomes more and more turbulent with increasing Reynolds numbers. The coefficient of surface drag, c_{dS}, of such shapes is high (Fig. 9d). The whole surface S is taken for area of comparison in the defining formula for this coefficient (see above). On the contrary, flow around bodies which are covered by such an "artifical dolphin skin" of optimal stiffness is partly laminar at the same Reynolds numbers. At very high Reynolds numbers the strange situation may occur, that flow is nearly fully laminar, if Kramer's extrapolation (see Fig. 9d) holds. Thus the coefficient of surface drag might well be reduced by one order of magnitude! It is highly probable that this is the answer to Gray's paradox.

Yet another of nature's creations is being put to use in technical science. Fish slime consists of long thread-like macromolecular colloid structures which are metabolically synthesized as protein chains or as long chains of slimy mucopolysaccharides. The effects of this slime were at first reported on by Toms (1948) and later by the American researchers Rosen and Cornford (1971), followed by others such as Hoyt (1975), who have shown that this slime greatly reduces friction drag in fish, e.g., by 66% in barracudas under the experimental conditions shown in Fig. 10. Figure 10a shows that drag reducing properties can be found in all possible types of natural and artificial polymers. As was to be expected, extremely favourable values were obtained with fish slime. The efficiency increases very rapidly at first when minimal quantities are added to sea water; maximum efficiency is achieved already with a "solution" of a few percent. Further increases in concentration do not bring improvement, but even cause a slight decrease in efficiency (Fig. 10b). Probably only the laminar sublayer directly under the actual boundary layer will have to be filled with slime particles in order to render the mechanism effective. If one calculates the slime production capacity of a fish one finds that a fish is able to produce sufficient slime in very short a period of time so that drag is reduced during occasional, short bursts of rapid swimming. Fish slime is hydrodynamically effective only directly after secretion. It degenerates very rapidly under the influence of enzymes and bacteria, thus losing its effectivity. One can picturize a kind of boundary layer "greasing" taking place when the long molecular filaments roll up and reduce the friction between the body surface and the immediately surrounding liquid film. Such positive effects occur only at high Reynolds numbers, i.e., at very high speeds such as a fish requires when shooting forward to trap prey or during escaping manoeuvers. Then and only then is it worthwhile to secrete slime. It would appear that drag reduction due to slime has been evolved by fish purely for cases of emergency, since it is only produced then when top speeds are required for short periods. Artificial "fish slime" can be synthesized. A product called Polyox, when mixed with the water used by fire

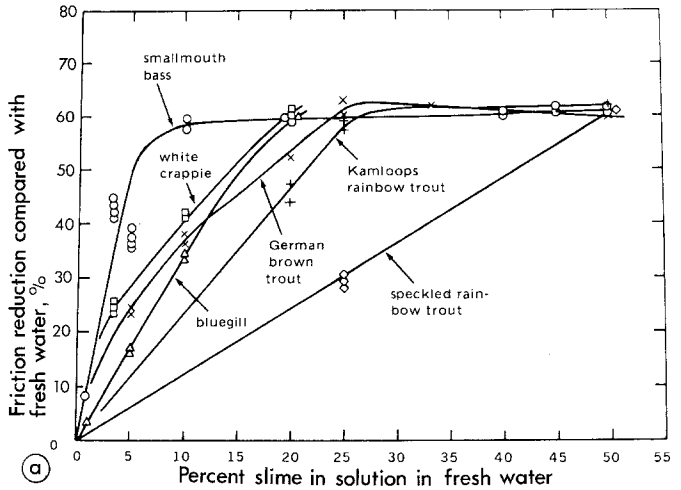

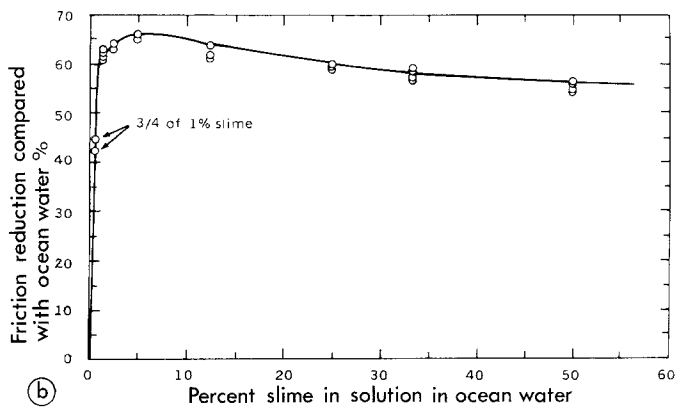

Fig. 10. a Drag reduction of flow in a narrow tube after the addition of several natural and synthetic slimes at various concentrations. **b** Dependence of drag reduction on the concentration of barracuda slime, determined by means of a rheometer. **a** and **b** According to Hoyt (1975) and Rosen and Cornford (1971), respectively

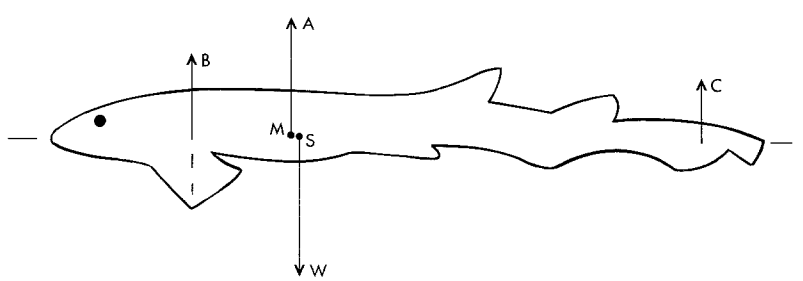

Fig. 11. Compensation of the moment of pitch in a shark. If the perpendicular distances of the forces A, B, C from the center of gravity S (which lies behind the metacenter M) are a, b, and c, then the balancing of the moments of pitch are $Aa + Bb = Cc$. The fin not only has to produce thrust, but also lift C. According to Alexander (1965)

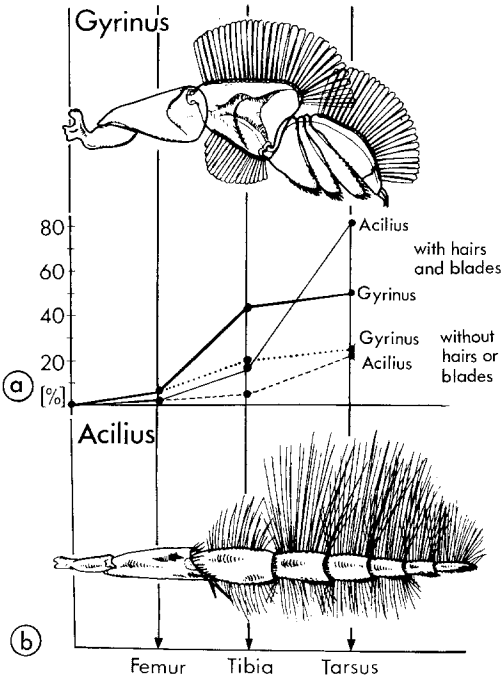

Fig. 12. The rowing legs of the medium sized water beetle *Acilius sulcatus* (**a**) and the smaller whirling beetle *Gyrinus substriatus* (**b**), redrawn to the same size. The %-distribution of drag (thrust) over the leg is indicated. According to Nachtigall (1961)

brigades, increases the length or height of the water jet at a certain pressure from the pumps and a certain length of hose. Four kilos are sufficient for 4,000 l of water which in turn are sufficient to extinguish an average sized fire. The momentary market price for this product is approximately DM 50.00 per kilo, an ingenious means of making good use of one of nature's effects!

Swimming animals make use of different types of appendages to create the thrust necessary to compensate for body drag. When swimming at a constant speed, their drag d is equal to thrust th. This can be said to hold for organisms which have rigid bodies and are propelled by moving appendages, e.g., water insects. Since buoyancy is usually a passive act (air bladder; only in sharks "dynamic lift" is generated, Fig. 11), muscle activity is reserved for propelling the animal forwards. Such a specialization has its advantages and has been very well developed by *Dytiscidae* and *Gyrinidae,* two water beetle families which have been studied by the author. Apart from the delicate steering muscles of the leg, there are only two groups of very strong propelling muscles in the thorax, one functional abductor which pulls the rear swimming legs very quickly backward and one functional adductor which draws the legs forward.

Swimming legs are very effective hydrodynamical thrust generators. The external parts of the legs, i.e., the tibia, and the tarsal parts, are extremely flattened, especially so in *Gyrinidae* (Figs. 12a and b). Dytiscidae have round swim hairs along the edges of their legs (Fig. 12a), and *Gyrinidae* have delicate "swimming laminae" which overlap at the base like playing cards (Fig. 12b).

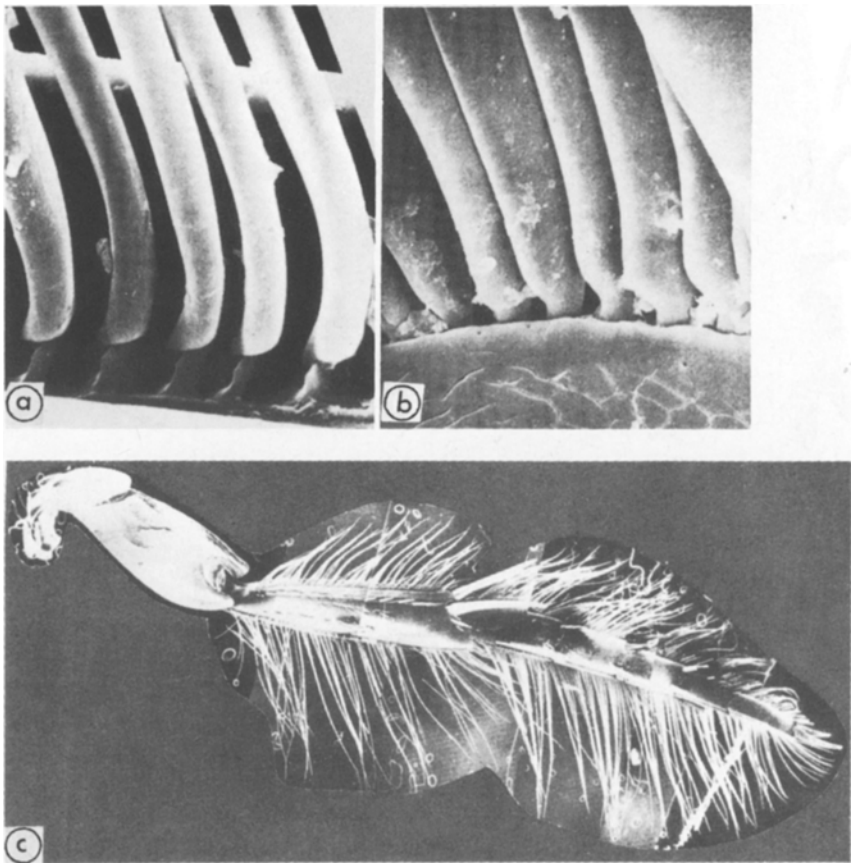

Fig. 13. a Articulation of the swimming hairs in *Acilius*. **b** Articulation of the swimming blades in *Gyrinus*. **c** Collage of single REM pictures of the Acilius rowing leg. According to Nachtigall (1970)

During a forward propelling paddle stroke, the legs are turned broadsides to the flow with the hairs and laminae stretched to a maximum. The latter is activated by flow pressure in less than a thousandth of a second. Hairs and laminae do not have muscles of their own, but have a refined slanting articulation (Figs. 13a and b). Whilst stretching they turn slightly and finally, when they come in contact with a common edge, they fling in one plane. The surface of the legs is immensely increased during paddle stroke (Figs. 13c, 14a parts 9, 10). When the legs are drawn forward, the swimming appendages are completely attached to the leg surface. Some parts of the leg lie in special grooves in their neighbouring part, so that the leg is trussed to form a very small and slender structure (Fig. 14a, parts 2, 3). $d \sim A r^2 \omega^2$ is valid for flow drag d; $th \sim c_d A r^2 \omega^2 \sin\alpha$ is valid for thrust th (c_d coefficient of leg drag, A leg surface area perpendicular to flow, r rotational distance from A, ω angular speed, α angle between leg length axis and middle line of the animal). d must have the largest possible value for the

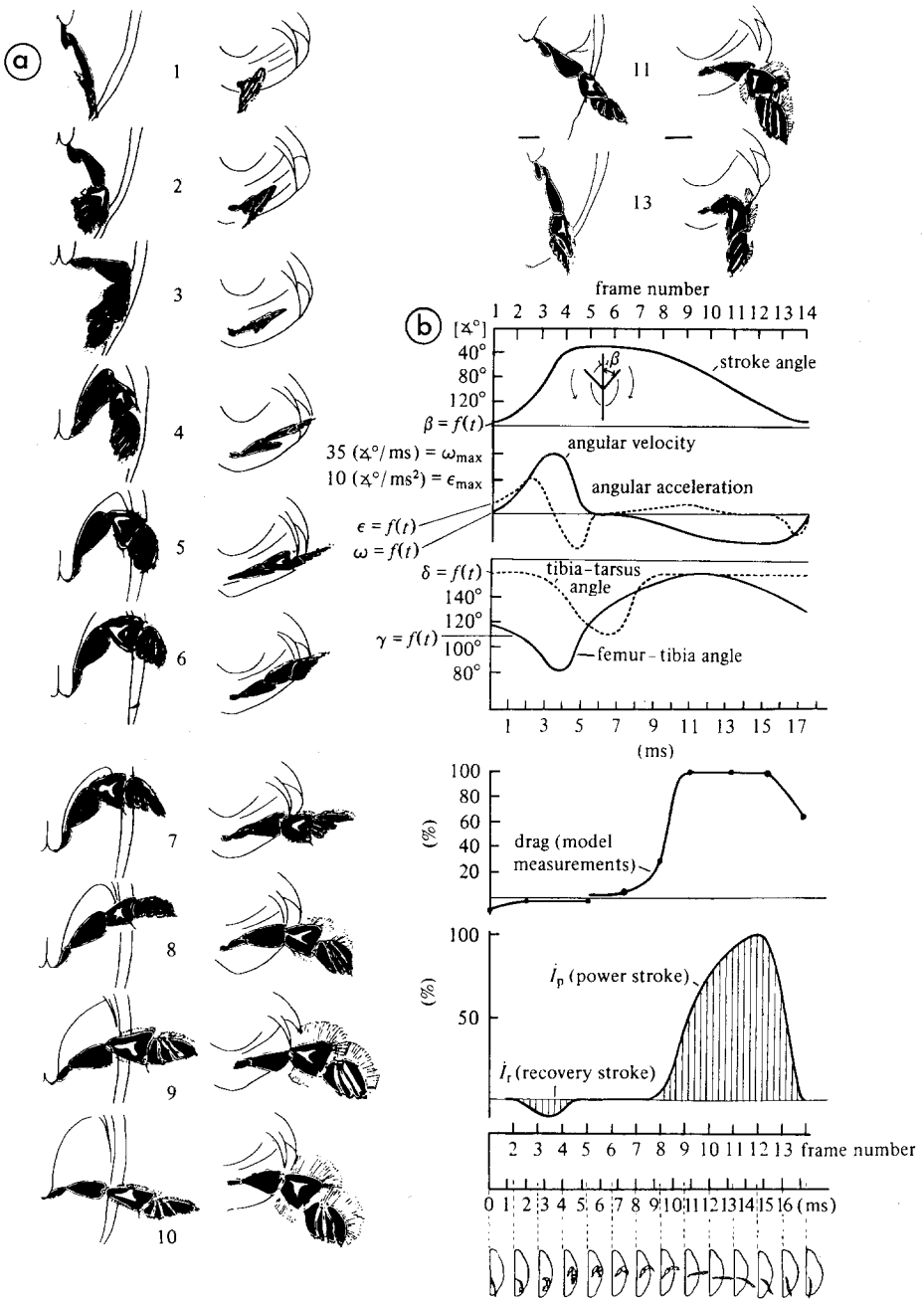

Fig. 14. **a** Course of a hindleg (rowing leg) stroke of the whirling beetle *Gyrinus substriatus*, seen from below and behind. **b** Kinematical and dynamical graphs to **a**. See text for explanation. According to Nachtigall (1961). **c** Drag of a model row made of 10 parallel "swimming hairs" (needles) as a function of their distance. Preliminary measurements from Nachtigall, unpublished

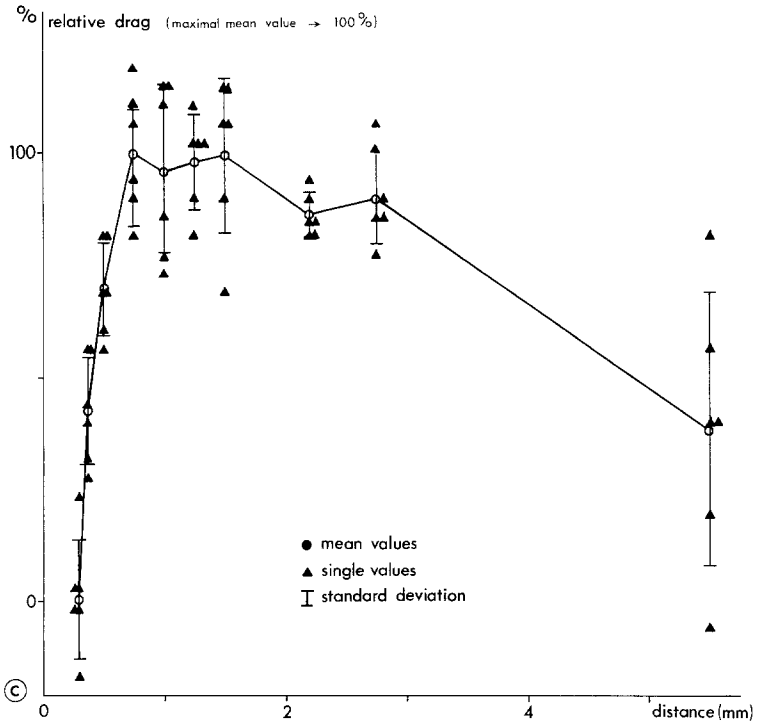

Fig. 14c. Legend see page 14

power stroke and the least possible value when the legs are drawn forwards. If *d* and *th* had the same value, then the animal would move back and forth on the same spot without advancing at all. Figure 14a shows high frequency pictures of the leg movements of *Gyrinus substriatius* taken from two different directions. Figure 14b shows several kinematic data. The areas below the base curve represent the time integrals of the forces in swimming direction, i.e., the "force impulses" or the change in thrust and counter thrust impulses. Graphical analysis shows that drawing forward of the legs only generates one fortieth of the drag of a rudder stroke. Hydromechanical degrees of efficiency of $\eta = 0.87$ are achieved; total hydrodynamic efficiency is smaller. *Gyrinus* legs surpass all technical structures as thrust generators using the drag principle and even attain efficiency of adjustable propellers which work on the hydrodynamically more favourable lift or side force principle.

Recent measurements made by my research team have shown that the swimming hairs may have reached a kind of hydromechanically optimal state in the relationship between their thickness and distance from one another. The preliminary conclusion is that they seem to stand, compared to their thickness, exactly so far apart that they generate – according to flow interference – maximum drag with a given volume (Fig. 14c).

When a fish with body length L swims forward, each point on its tail fin follows a sinus path with a wave length λ_S (Fig. 15). A so-called "metachronical body wave" moves simultaneously in the opposite direction. This wave has the

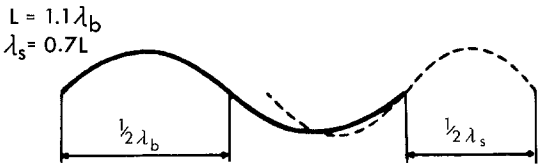

Fig. 15. Diagram of the relationship between body length L and wave length λ of a fish swimming at "average top speed". According to Wardle and Videler (1980)

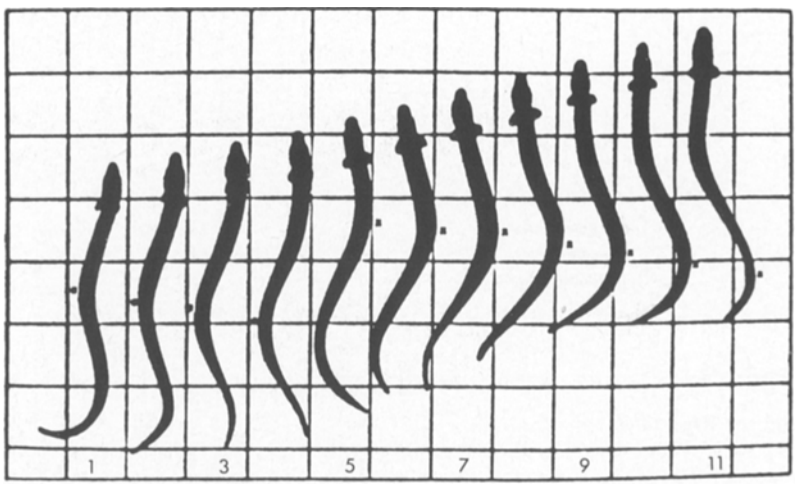

Fig. 16. Drawings of the long fish Centronotus gunnelus from films. The distance between grids is 25 mm, the time between drawings is 0,05 s. According to Gray (1968)

Fig. 17. Motion phases of the mackerel *Scomber scombrus*. Length 0,37 m, photo frequency 0.01 s, swimming speed 2.83 ms^{-1}. Photos from television screen. According to Wardle and Videler (1980)

length $\lambda_K \geq \lambda_S$. An increase in the amplitude of this wave towards the tail is even more apparent in long, slim fish (Fig. 16). This results from the contracting muscles along the sides of the fish and the speed w of the metachronical wave is always slightly greater than the swimming speed v of the fish. Since both waves have a common period of duration, $v : w = \lambda_S : \lambda_K$. The relation $\lambda_S \approx 0.7\ L$ is a good approximation for many fish. This can be deduced from Fig. 17 which shows a mackerel (*Scomber scombrus*), photographed by Wardle and Videler with a special television camera. If this relationship is valid, then the maximum swimming speed v_{max} of a fish can be determined when the shortest time of contraction t_K of the (white) swim muscles of one side of the fish is known: $v_{max} = 0.7\ L/2\ t_K$. In a large, 80 cm long fish e.g., $t_K = 0{,}05$ s and therefore $v_{max} = 5.6$ m/s^{-1}. However, this speed can only be held for very short periods of time.

Fish often move forwards by moving their tail fins to and from. Hertel has shown that this type of movement consists of two oscillations similar to that of the fluttering of aeroplane wings (Fig. 18a). These two oscillations, mentioned above, a "bending oscillation" and a rotational oscillation, are coupled by a phase angle of 90°. If one now observes how the tail fin of a trout is positioned relative to the direction of its movement (Fig. 18b), it will be seen that forward driving components result from almost every position and add up to total thrust during a whole period. This display of forces resembles that of beating bird wings as shown in Fig. 18c where the wing is thought "frozen" perpendicular to the paper plane. Stationary force analysis shows that a drag component in the direction of movement and a transverse force component perpendicular to it ("lift") give rise to a resultant which can be divided into a forward driving component, thrust, and a vertical force component. The latter prevents a bird from falling. During tail fin beating in fish, these components, known as lateral forces, change direction every half beat. The sum of these lateral forces is zero in forward swimming, whilst the forward driving components show in swimming direction all the time (Fig. 18d). A trout's fin can only achieve a favourable position to its path of movement when it not only rotates, but also moves to the left and to the right side in a transpository manner. Both these components must play together with a favourable phase shift. As it has been mentioned above the ideal phase shift is 90°, and 72° have been measured in a swimming trout by Hertel (Fig. 18e). Values around 70° have been confirmed by new analyses of trout swimming, made by the author (yet unpublished). So the measured value is relatively close to the ideal value.

Let us now reconsider the dependence of moving organisms on the Reynolds number (Fig. 1). Especially in the intermediate zone, i.e., theoretically at Reynolds numbers around one (and pratically at values which are an order of magnitude larger), interesting effects should appear. At this Reynolds number the force of inertia is more or less equal to the force of viscosity. At higher Reynolds numbers, such as 10^2 to 10^3, the inertial forces are largely predominant. Nature and technical science make good use of them. It does not matter whether the animals swim in water or fly in the air; both can be treated as fluids and one can compare them under flow dynamic aspects. As can be seen in Fig. 19, lift is still about three times greater than drag in butterflies' wings at

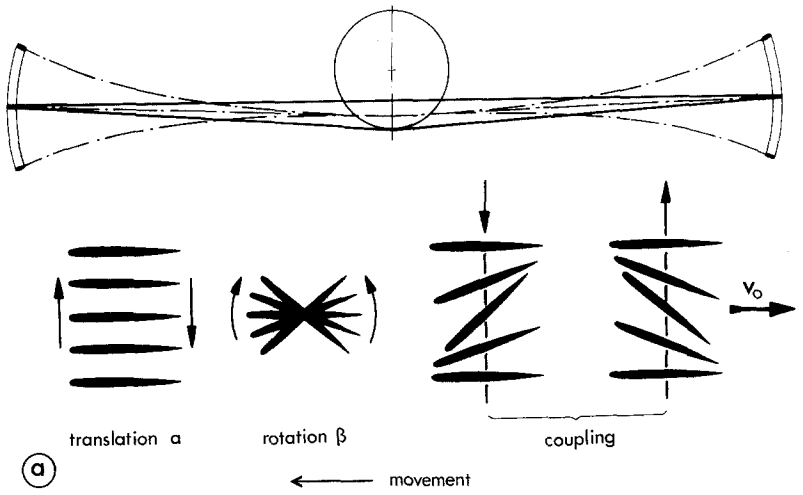

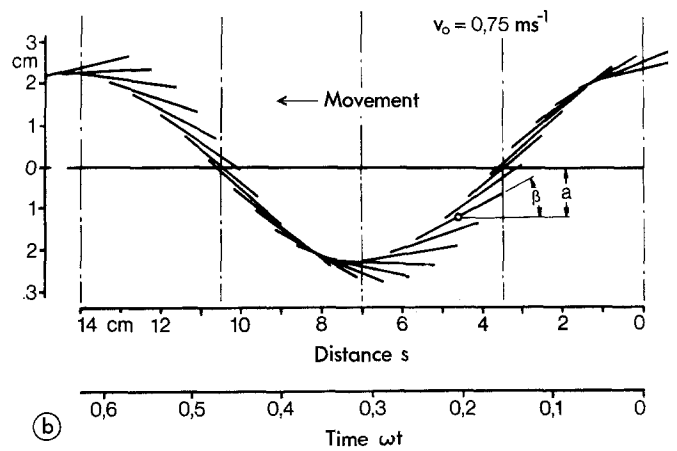

Fig. 18. a Wing fluttering explained as a combination of two oscillations with a phase angle of $\varphi = 90°$. After Hertel (1963). **b** Tail fin stroke of a trout: kinematical curve. The angle of the tail fin to path direction and the distance a of the central point of the tail fin from the center axis is indicated. After Hertel (1963). **c** Forces produced during down stroke by a birds wing. After Nachtigall (1976). **d** Diagram of forces from tail fin stroke from a trout. After Hertel (1963). **e** Sinusoidal time functions of translation and roation movements of a trouts tail fin. There is a phase shift of 72°. After Hertel (1963)

(relatively small) Reynolds numbers around 10^3. So flying and swimming following the principles of lift resp. lateral forces, appear to be significant when the wings or fins are obliquely positioned to the direction of flow, so that maximum lift will be created. In butterflies this seems to be around $+10°$ as shown in Fig. 19. At lower Reynolds numbers the lift-drag relation decreases rapidly (Fig. 20) and begins to reverse itself at $Re \approx 50$. With continued

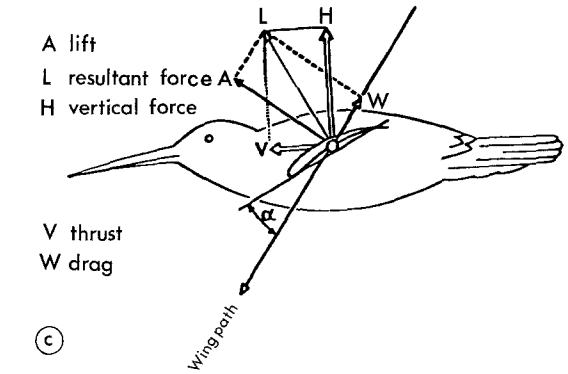

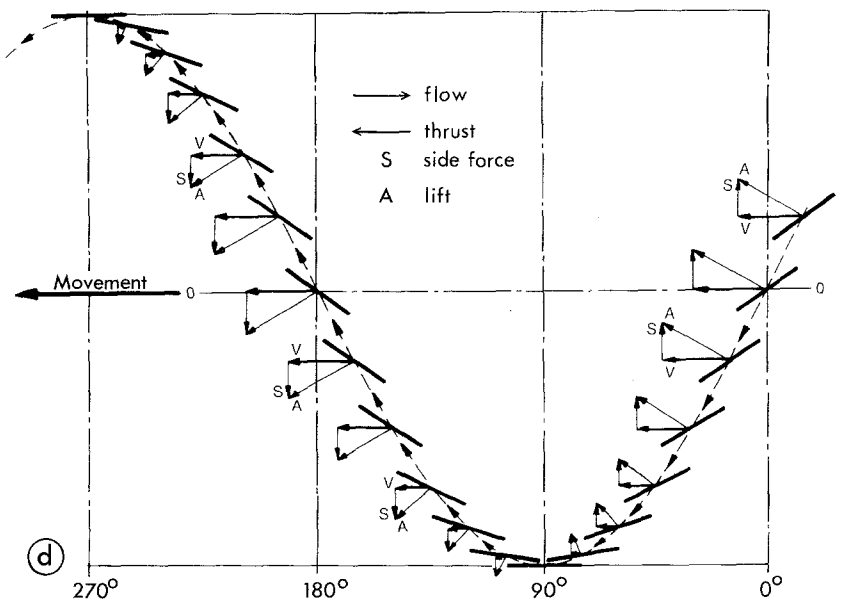

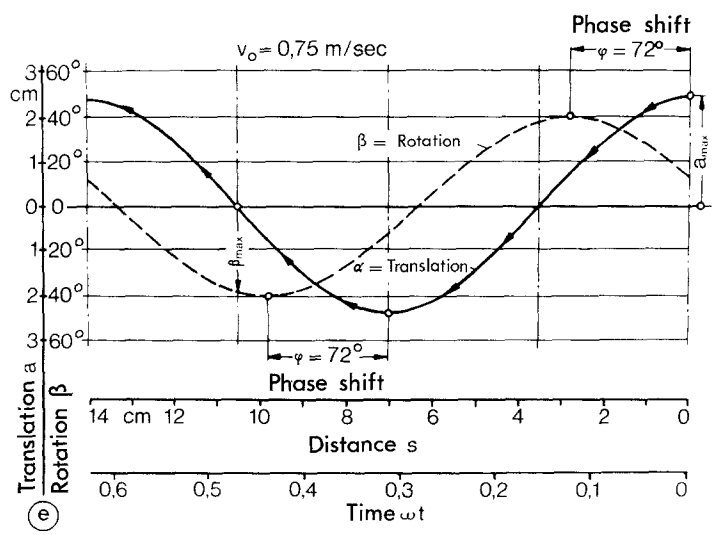

Fig. 18c–e.
Legend see page 18

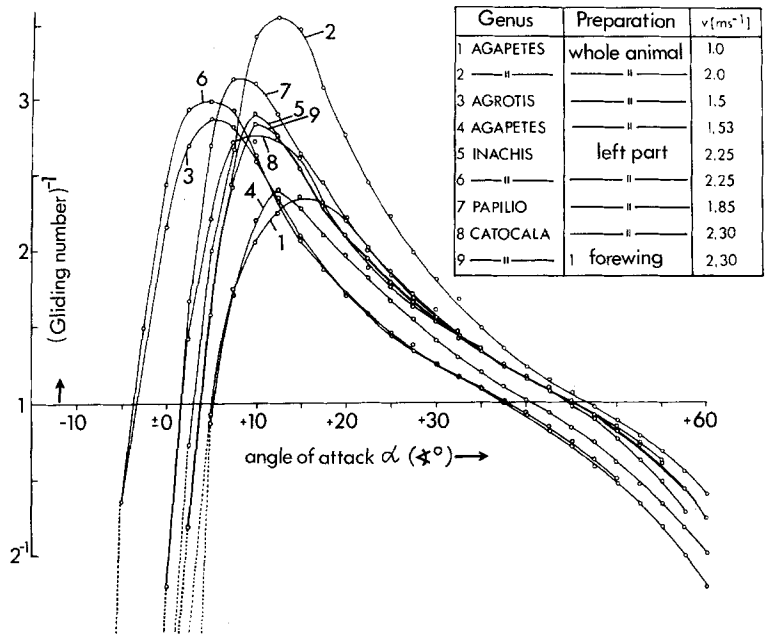

Fig. 19. Reciprocal value of the gliding number, c_A/c_W, as a function of the angle of attack, plotted for the forewings of nine butterfly species (see indications inserted); Re $\approx 10^3$. According to Nachtigall (1967)

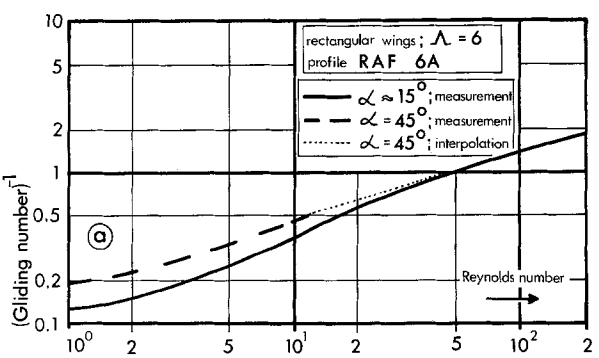

Fig. 20. Dependence of the reciprocal value of the gliding number, c_A/c_W, on Reynolds number for rectangular wings of small aspect ratio. According to Thom and Swart (1940)

reduction of the Reynolds number drag becomes greater than lift. Evolution has complied with these flow dynamic conditions. Whilst insects flying at Re $\approx 10^3$ still have "conventional" wings resembling flat or gently cambered plates which work optimally in this range of Reynolds numbers (dragonflies, Fig. 1; butterflies, Fig. 19), smaller insects flying at Re $\leqslant 10$ look quite different. Their wings are club shaped stumps surrounded with a fringe of bristles lying in one plane (Figs. 1 and 21). They seem to function almost like the legs of water beetles (Fig. 12a), mainly following the principles of drag: for such small insects, air is a viscous medium in which they paddle around just like water beetles in water! A convincing indication of the real validity of this principle lies in the

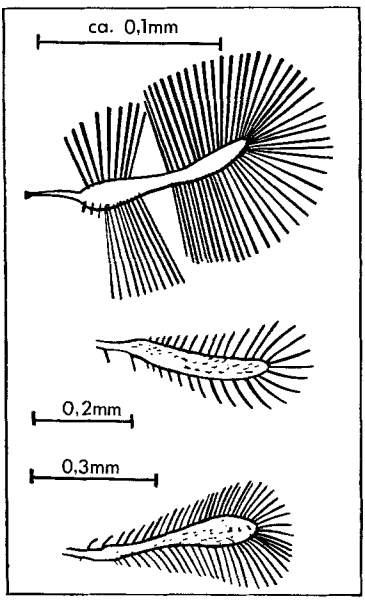

Fig. 21. Wing shapes in various very small insects. Top to bottom: beetle, thrips, parasitic Hymenopterau. According to various authors from Nachtigall (1978)

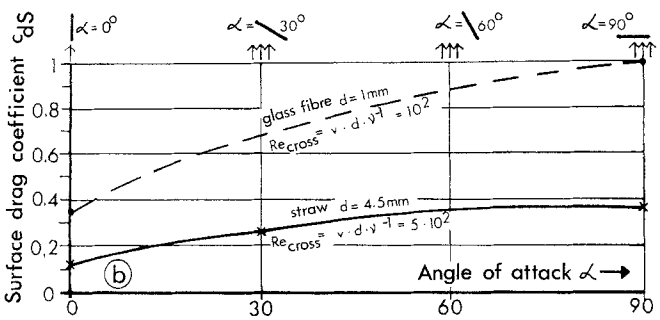

Fig. 22. Dependence of the surface drag coefficient c_{dS} on the angle of attack α of filamentous structures. Reynolds number approx. 10^2. According to Hertel (1963)

fact that specimens with bristly club shaped wings resembling water beetle legs are to be found in different insect groups, e.g., tiny beetles, hymenoptera, and thrips (Fig. 21). It is not necessary that this kind of wing should be angularly exactly adjusted in relation to the stroke path, as it is the case with the wings of flies and dragonflies. As can be seen in Fig. 22, the surface drag coefficient c_{dS} does not alter much even at ernormous changes in the angles of attack between 0° and 90°. Considering the range of relevant angles of attack in butterflies and dragonflies which lies between a few degrees and perhaps 30°, the difference in c_{dS} of the tiny wings will reach at the most the factor 2. Therefore such "bristle wings" do not have to be precisely pitched and just have to be brought into contact with the air somehow or other. Thus it can be expected that these small insects do not possess as complicated wing kinematics as do larger insects.

Hydromechanics and biology complement one another. On the one hand, knowledge of hydro- and aerodynamics will help the biologist to analyze correctly and better understand the biological structures he is dealing with. On the other hand, nature's constructions may stimulate the hydrodynamicist in the development of his own constructions with respect to greater efficiency as well as to making optimal use of materials.

Acknowledgement. I wish tho thank Mrs. W. Pattullo for the translation of the manuscript.

References

Hertel H (1963) Biologie und Technik. Struktur, Form, Bewegung. Krausskopf, Mainz

Nachtigall W (1977) Zur Bedeutung der Reynoldszahl und der damit zusammenhängenden strömungsmechanischen Phänomene in der Schwimmphysiologie und Flugbiophysik. In: W. Nachtigall (Hrsg) Physiology of movement – biomechanics. Symposium Mainz 1976. Fortschr. Zool. 24: 13–56

Nachtigall W (1980) Mechanics of swimming in water-beetles. In: Elder HY, Trueman ER (eds) Aspects of animal movement. Sem. Series 5. Cambridge University Press, Cambridge, pp 107–124

Wardle CS, Videler JJ (1980) Fish swimming. In: Elder HY, Trueman ER (eds) Aspects of animal movement. Sem. Series 5. Cambridge University Press, Cambridge, pp 125–150

More literature especially in Nachtigall (1977) and Wardle and Videler (1980)

Received August 13, 1981/Accepted September 28, 1981